Science of the Total Environment 753 (2021) 141768

Contents lists available at ScienceDirect

Science of the Total Environment

journal homepage: www.elsevier.com/locate/scitotenv

Sunlight-induced changes in naturally stored reclaimed water: Dissolved organic matter, micropollutant, and ecotoxicity

Yongkun K. Wang, Xiaoyan Y. Ma, Shiying Zhang, Lei Tang, Hengfeng Zhang, Xiaochang C. Wang *

International Science & Technology Cooperation Center for Urban Alternative Water Resources Development, People's Republic of China
Key Lab of Northwest Water Resource, Environment and Ecology, MOE, People's Republic of China
Engineering Technology Research Center for Wastewater Treatment and Reuse, Shaanxi Province, People's Republic of China
Shaanxi Key Laboratory of Environmental Engineering, Xi'an University of Architecture and Technology, Xi'an 710055, People's Republic of China

HIGHLIGHTS

- Effects of sunlight on RW during open storage were assessed at different seasons.
- Sunlight-induced changes of CDOM absorption and FDOM components were analyzed.
- Sunlight-induced attenuation of 52 residual micropollutants in RW was explored.
- Detected micropollutants explained 0.02–2% of ecotoxicity variations.
- CDOM and FDOM were significant correlation with the reduction of ecotoxicity.

GRAPHICAL ABSTRACT

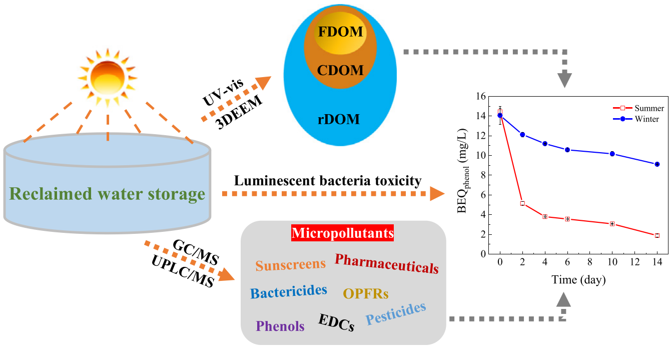

ARTICLE INFO

Article history:
Received 5 July 2020
Received in revised form 14 August 2020
Accepted 16 August 2020
Available online 18 August 2020

Editor: Shuzhen Zhang

Keywords:
Reclaimed water storage
Natural sunlight
Dissolved organic matter
Micropollutant
Luminescent bacteria acute toxicity

ABSTRACT

Natural sunlight is a vital environmental element and plays a significant role in the ecological storage of reclaimed water (RW), but its impacts on RW quality are poorly understood. In this study, sunlight-induced changes in RW with a focus on dissolved organic matter (rDOM) and 52 residual micropollutants were investigated in the field during the summer and winter seasons. The results indicated that sunlight exposure led to the dissipation of chromophoric DOM (CDOM) in the summer (55% loss) and winter (19% loss) after 14 consecutive sunny days. During open storage of RW, CDOM absorption in UVC regions was preferentially removed in the summer, while during the winter there was preferential removal of CDOM in UVA regions. The results also showed higher fluorescent DOM (FDOM) removal in summer than in winter (49% and 28%, respectively). Results in both seasons indicated that humic acid-like compounds were the most photolabile fractions and were preferentially removed under sunlight exposure. Sunlight also induced attenuation of micropollutants in the summer and winter at reductions of 66% and 24% from the initial values, respectively. Significant attenuation (>75%) was only observed for endocrine-disrupting chemicals, pharmaceuticals, and sunscreens in the summer, but they accounted for 76% of the total concentrations. *Vibrio fischeri* toxicity tests demonstrated that sunlight constantly decreased the luminescent bacteria acute toxicity of RW, which was estimated to be caused mainly by the sunlight-induced changes of FDOM and CDOM, while the detected micropollutants could only explain 0.02%–2% of acute toxicity. These findings have important implications regarding our understanding of the ecological storage of reclaimed water and the contribution of management strategies.

---

* Corresponding author.
E-mail address: xcwang@xauat.edu.cn (X.C. Wang).

https://doi.org/10.1016/j.scitotenv.2020.141768
0048-9697/© 2020 Elsevier B.V. All rights reserved.

1. Introduction

Reclaimed water from municipal wastewater has become an accessible and reliable water source to mitigate growing water shortages (Lyu et al., 2016; Shannon et al., 2008). In terms of reclamation and reuse, storage is a critical part of the process due to hourly and seasonal variations in demand for reclaimed water supply (Miller and Quinlan, 2003). Reclaimed water can be stored in open spaces such as reservoirs, lakes, or open-air ponds. These storage units have also been used as environmental buffers, which could further expand the spatial scale of water purification and enrich and strengthen the resource attributes of reclaimed water (Hu et al., 2018; Ma et al., 2016; Sun et al., 2016). The quality of reclaimed water is the most important consideration for reuse applications, particularly with regard to the organic components (Hu et al., 2016; Michael-Kordatou et al., 2015; Miller and Quinlan, 2003). However, water quality may be changed during open storage due to various natural processes such as sorption, hydrolysis, biodegradation, volatilization, and photolysis (Hawker et al., 2011; Lv et al., 2017; Ma et al., 2016; Sun et al., 2016).

Owing to its unique origins, organic components present in the reclaimed water mainly consist of two major types of components: macromolecular dissolved organic matter (DOM) and micromolecular organic micropollutants (Hu et al., 2016; Michael-Kordatou et al., 2015). Since the storage of reclaimed water may be long-term or seasonal, natural sunlight irradiation is believed to play an important role in transforming reclaimed water DOM (rDOM) and as well as the attenuation of micropollutants (Bahnmuller et al., 2014; Wang et al., 2017; Yang et al., 2014; Du et al., 2017; Du et al., 2018a, 2018b). Upon exposure to photo-irradiation, the photochemical transformation of DOM, particularly chromophoric DOM (CDOM) and fluorescent DOM (FDOM), can be induced by direct photolysis and indirect photoreactions. It has been shown that sunlight irradiation can alter the physico-chemical properties of the DOM by altering parameters such molecular weight distribution, conformation, and DOC contents (Q. Wu et al., 2016; Q.-Y. Wu et al., 2016). These processes are otherwise known as photobleaching and photomineralization (Niu et al., 2014).

Micropollutants remaining in reclaimed water may undergo photolysis during open storage (Ma et al., 2018). Micropollutants from domestic wastewater are at low concentrations (usually in the level of ng/L) and are highly complex (Pereira et al., 2017). The occurrence of micropollutants, e.g., endocrine-disrupting chemicals (EDCs), pesticides, pharmaceuticals, and sunscreens, has been reported worldwide (Hu et al., 2016; Michael-Kordatou et al., 2015). Studies reported that micropollutants can be degraded not only by direct photolysis when their absorption spectra overlap with the solar irradiation spectrum but also by indirect photolysis through reactions with photochemical reactive intermediates (PPRIs) formed by the sunlight excitation of photosensitizers (Vione and Scozzaro, 2019; Wang et al., 2017). In terms of reclaimed water that is stored in open reservoirs for 7 days or more (Cirelli et al., 2008; Miller and Quinlan, 2003), the impacts of natural sunlight on residual micropollutants are still unknown. To date, numerous studies have focused on sunlight-induced changes in DOM or micropollutants in various waters such as natural waters, treated effluents, and their mixtures in laboratory experiments (Bodhipaksha et al., 2017; Ge et al., 2019; Sardana et al., 2019; Q. Wu et al., 2016; Q.-Y. Wu et al., 2016; Zhang et al., 2019), while limited research has been devoted to exploring the sunlight-induced changes in DOM or micropollutants in the field. The results of laboratory experiments, with different simulated solar light and micropollutant concentrations (e.g., several orders of magnitude above those found in real wastewater), may be inadequate for environmental applications (Wang and Lin, 2014). Additionally, natural solar light demonstrates daily and seasonal variability, and the fractions of organics in treated effluents also fluctuate (Hu et al., 2016; United Nations Environment Programme, 2016). Hence, investigating the impacts of natural sunlight irradiation on organic components under field conditions is of great importance for gaining an understanding of the function of ecological storage and determining the fate of hazardous substances.

Storage of reclaimed water in open spaces such as in open-air ponds and lakes increases detoxification (Ma et al., 2016). Reclaimed water sources still exhibit high estrogenic activity, genotoxicity, or cytotoxicity, which is like to endanger aquatic ecosystems (Hu et al., 2016; Jia et al., 2015). During the open storage of reclaimed water, sunlight-induced changes in hazardous substances would play a significant role in the evolution of biotoxicities (Du et al., 2018a, 2018b; Lv et al., 2017; Q. Wu et al., 2016; Q.-Y. Wu et al., 2016). Lv et al. demonstrated that solar light irradiation significantly reduced cytotoxicity in reclaimed water (Lv et al., 2017). However, Wang et al. indicated that the natural purification process of sunlight exposure would increase the bacterial cytotoxicity of mixtures of pharmaceuticals in wastewater treatment plant (WWTP) effluents owing to phototransformation byproducts (Wang and Lin, 2014). There is a need to identify the role of natural sunlight in the evolution of biotoxicity during the open storage of reclaimed water (Giannakis et al., 2016; Jasper and Sedlak, 2013).

The aim of this study was to determine the effects of natural sunlight on rDOM and residual micropollutants during the open storage of reclaimed water. UV–visible spectroscopy (UV–vis), three-dimensional excitation-emission matrix fluorescence spectroscopy (3DEEM), and liquid chromatography were employed to reveal the changes in rDOM, while the attenuation behaviors of residual micropollutants with environmentally realistic concentrations (including EDCs, pharmaceuticals, sunscreens, pesticides, bactericides, organic phosphorus flame retardants (OPFRs), and phenols) were revealed using instrumental analysis. The evolution of biotoxicity (*Vibrio fischeri*) of the reclaimed water mixture was also examined, and the mechanisms of sunlight-induced detoxification were discussed in depth.

2. Materials and methods

2.1. Chemicals

The standards that were used in this study consisted of 52 micropollutants, which were purchased from AccuStandard (New Haven, CT): estrone (E1), estriol (E3), 17-alpha-Estradiol (αE2), 17-beta-Estradiol (βE2), 17a-ethinylestradiol (EE2), bisphenol A (BPA), naproxen (NPX), mefenamic acid (MEF), ibuprofen (IBU), roxithromycin (ROX), sulfamethoxazole (SMX), trimethoprim (TMT), clarithromycin (CLR), erythromycin (ERY), ketoprofen (KPF), carbamazepine (CBZ), diphenhydramine hydrochloride (DPH), fluoxetine hydrochloride (FLX), benzophenone-1 (BP1), oxybenzone (BP3), 2-benzoyl-5-methoxy-1-phenol-4-sulfonic acid (BP4), 4-aminobenzoic acid (PABA), octocrilene (OC), 2-ethylhexyl 4-dimethylaminobenzoat (OD-PABA), avobenzone (BM-DBM), octyl 4-methoxycinnamat (EHMC), simazine (SMZ), atrazine, cyanazine (CYZ), prometryne (PRT), ametryn, terbuthylazine (TET), dichlorvos (DDVP), triallate (trt), trichlorfon (TRF), acetamiprid (ACT), imidacloprid (IMP), thiamethoxam (Thixam), carbendazim (CBM), prochloraz (PCL), azoxystrobin (Azobin), dimethomorph (DMM), difenoconazole (DFZ), triadimefon, tris(2-Chloroethyl) phosphate (TCEP), triphenyl phosphate (TPhP), triphenylphosphine oxide (TPPO), tributyl phosphate (TBP), tris(1-chloro-2-propyl) phosphate (TCPP), phenol, p-Cresol, 2,4,6-trichlorophenol (2,4,6-TCP). Probe compounds of furfuryl alcohol (FFA, 98%), 2,4,6–trimethylphenol (TMP, 99%), terephthalic acid (TA, 98%) and 2-Hydroxyterephthalic acid (2HTA, 98%) were purchased from J&K Scientific (China). Solvents were of HPLC grade (Fisher Scientific), and ultrapure water (18.2 MΩ·cm) was generated with a Millipore Ultrapure Water System (Milli–Q® Biocel®). All the other reagents used were of analytical grade or higher.

2.2. Storage conditions

2.2.1. Experimental-setup and operation

Experiments were performed using reclaimed water from a wastewater treatment plant located in Xi'an China (lat. 34°14′03″N, 109°04′09″E). An anaerobic-anoxic-oxic unit followed by a membrane bioreactor (A^2O-MBR) process was employed in the WWTP to treat domestic wastewater (Ma et al., 2016). The effluent quality of this treatment system complied with relevant standards for reclaimed water reuse (SL368-2006: Standards of Reclaimed Water Quality). The generated reclaimed water was stored in the main storage tank and then sent to replenish an artificial landscape lake, and further used for various non-potable purposes. Reclaimed water for the present experiments was collected from the main storage tank. Table S3 shows the average values and standard of the reclaimed water parameters used in the experimental period. During each season, the reclaimed water samples were collected from the WWTP once every two weeks for residual micropollutant analysis ($n = 4$).

In the current study, an open-air storage pond was constructed in the open-air space of the local WWTP, with the dimensions of 2.4 m in length and 1.8 m in width. After immersion cleaning, reclaimed water from the main storage tank was pumped into the pond, and the depth of the pond water was set at 0.5 m. We studied the sunlight-induced changes in the reclaimed water under real-world conditions over two contrasting seasons. During the summer exposure period, outdoor experiments were carried out over 14 consecutive sunny days under ambient temperatures during the days and at night. The air temperature was generally in the range of 16–31 °C. During the winter exposure period, the air temperature was generally in the range of −3–7 °C, and the experiment was carried out over the same interval as during the summer season. The environmental conditions were typical for the corresponding season of the year at this location. The evaporation loss was recorded and no rainfall occurred throughout the whole experimental period.

2.2.2. Solar radiation measurement

Natural sunlight intensity variations with wavelengths of 275–320 nm, 320–400 nm, and 400–1000 nm were monitored using UV-B, UV-A, and FZ-A irradiance meters, respectively (Beijing Normal University Photoelectric Instrument Factory, Beijing, China). The average solar irradiance during the exposure period during different seasons is presented in Fig. S2. During the summer exposure period (solar elevation angle about 75°), the average intensities of incident visible light irradiances, UVA, and UVB were 495.7, 19.9, and 0.87 W/m^2, respectively. The corresponding diurnal solar energy accumulated per unit volume for the reclaimed water was calculated by Gaussian function (Text S1) and found to be 39.7, 1.6, and 0.07 kJ/L, respectively. During the winter exposure period (solar elevation angle about 32°), the average solar incident irradiances were weaker than during the summer. The average intensities of incident visible light irradiances, UVA, and UVB were 176.7, 5.9, and 0.21 W/m^2, respectively. The corresponding diurnal solar energy received per unit volume was found to be 14.1, 0.47, and 0.017 kJ/L, respectively.

2.3. Chemical analysis

2.3.1. Sample collection and processing

During each exposure period, approximately 5 L of reclaimed water was collected from the open-air storage pond in amber glass bottles every 2–4 days (between 10:00 and 11:00 am). The water sample was collected from the fixed water outlet which located 20 cm above the bottom of the storage pond. After that, the samples were taken to the nearby laboratory and filtered through a 0.7 μm glass microfiber filter (Φ150 mm; Whatman™) immediately. Dissolved organic carbon (DOC) concentrations in acquired samples were quantified using a total organic carbon analyzer (TOC-VCPN, Shimadzu, Japan). For each sample, 2–3 replicates were measured, giving a relative standard deviation of less than 2%.

In order to extract a wide range of contaminants from the samples for subsequent analysis, a solid-phase extraction (SPE) protocol based on the methods of Ma et al. (Ma et al., 2018) and Tang et al. (Tang et al., 2014) was adopted with some modifications. Briefly, filtered samples were acidified to pH 2.5 with 2 M H_2SO_4, and up to 5% methanol was added before extraction. The cartridges (Waters Oasis® HLB (500 mg, 6 mL)) were preconditioned with 10 mL dichloromethane: hexane mixture (1:1, v:v), 10 mL methanol, and 10 mL Milli-Q water in sequence. For micropollutant analysis, 2 L filtered samples were extracted using an extraction vacuum chamber (SUPELCO VISIPREP). The cartridges were dried completely under vacuum. They were then individually eluted with 10 mL of methanol and 10 mL of dichloromethane: hexane mixture (1:1, v:v) and were evaporated to 1 mL under purified nitrogen gas. Finally, 1 mL extracts with methanol solvent were used for UPLC-MS/MS analysis, and 1 mL extracts with acetone: hexane mixture (1:9, v:v) were used for GC–MS analysis. For luminescent bacteria toxicity test, the water sample was concentrated mainly following the SPE protocol of micropollutants analysis as described above. Briefly, 1 L filtered reclaimed water samples were extracted, and the obtained extracts were redissolved in 2 mL 1% dimethyl sulfoxide (DMSO) for luminescent bacteria toxicity test.

2.3.2. Spectroscopic characterization

UV–vis absorbance spectra of acquired samples were measured on a UV–visible spectrophotometer with a 1 cm path quartz cell (UV-1800, Shimadzu, Japan). Absorption spectra from 200 to 600 nm were scanned at 1 nm intervals. Total CDOM was calculated as the integrated absorption from 250 to 450 nm (Helms et al., 2008). E_2/E_3 was calculated using absorption coefficients at the corresponding wavelengths (250 nm and 365 nm). Absorption spectral slope ratios (S_R) have been defined as the ratio of the slope of the 275–295 nm region to the slope of the 350–400 nm region ($S_R = S_{275-295}/S_{350-400}$), which can be used to track the changes in the relative size of DOM molecules (Helms et al., 2008; Yang et al., 2014).

3DEEMs of various samples were recorded with a fluorescence spectrophotometer (F-7000, Hitachi, Japan), following a previous method (Hu et al., 2017). Fluorescence regional integration (FRI) was used to analyze the 3DEEM maps and divide them into four regions (F1, F2, F3, and F4) (Chen et al., 2003; Song et al., 2019); the description of each region is provided in Table S4. The FRI approach can make all of the fluorescence information in the EEM maps available and enables a comparison of different samples with quantitative fluorescence information. The EEM datasets were processed using Origin 2017 software. The EEM of Milli-Q water was used as a blank and to eliminate the Raman scatter. The effects of first-order and second-order Rayleigh scattering were removed using three-dimensional Delaunay interpolation.

2.3.3. Quantification of micropollutants

In the present study, 52 micropollutants were selected and monitored in the reclaimed water, and the photodegradation behavior of micropollutants in the open-air storage pond was examined during each seasonal exposure period. These targeted micropollutants included 6 EDCs, 12 pharmaceuticals, 8 sunscreens, 12 pesticides, 6 bactericides, 5 OPFRs, and 3 phenols (Table 2). Six analytical procedures were performed to quantify the chemicals in the acquired samples using a TSQ Quantum XLS (GC/MS, Thermo, USA) equipped with a DB-5MS (30 m × 0.25 mm × 0.25 m) capillary column and an ACQUITY UPLC-Xevo TQ MS (UPLC/MS, Waters, USA) equipped with an ACQUITY BEH C18 column (100 m × 2.1 mm × 1.7 m). Details of these analytical procedures can be found in previously published studies (Ma et al., 2018; Ma et al., 2019).

2.4. Bioanalysis

The bioluminescence inhibition assay with *Vibrio fischeri* was selected to detect the luminescent bacteria acute toxicity of reclaimed water mixtures before and after sunlight exposure. The toxicity test was conducted according to a modified ISO 11348 (2008) procedure (Ma et al., 2016). Briefly, a 100 μL prepared bacterial suspension was exposed to a 100 μL concentrated water sample with three replicates at every concentration in a microplate for 15 min. The relative light unit was then measured using Centro LIApc LB962 Microplate Luminometer (Berthold Technologies Company, Germany). The solution containing 1% DMSO and 2% NaCl was set as the negative control. The effective concentration (EC_{50}) was used to quantify the luminescent bacteria toxicity. To make the toxicity results comparable, the bioluminescence inhibition of different samples was standardized to the bioanalytical equivalent concentration (BEQ_{bio}) using a positive reference compound (phenol) (as Eq. (1) shown):

$$BEQ_{\mathrm{bio}} = \frac{EC_{50}(\mathrm{phenol})}{EC_{50}\ of\ water\ sample}, \tag{1}$$

2.5. Data analysis

The attenuation of targeted micropollutants during each exposure period was determined as the percentage of reduction between the concentration in the initial reclaimed water and the concentration after sunlight exposure. Water loss due to the evapotranspiration was considered, and the calculation of attenuation rate was as follows (Eq. (2)):

$$R(\%) = \left(C_0 - C_t\left(1 - \frac{t \cdot EVR}{V}\right)\right)/C_0 \times 100, \tag{2}$$

where C_0 is the initial concentration, and C_t is the concentration on each sampling campaign ($t = 0, 2, 4, 6, 10$, and 14 (day)). The average evaporation rates (EVR) are 22.5 and 8.9 L/d for the summer and winter exposure experiments, respectively. V is the total water volume of the open-air storage pond, 2160 L.

The redundancy analyses (RDA) method was utilized and carried out with Canoco for Windows 4.5. The graphics were created with CanoDrw4.

2.6. Acute toxicity prediction based on detected micropollutants

The effects of detected micropollutants on *V. fischeri* were predicted using the concentration addition (CA) model (Tang et al., 2013). The CA model is defined by Eq. (3):

$$EC_{50,CA} = \frac{1}{\sum_{i=1}^{n} \frac{p_i}{EC_{50,i}}}, \tag{3}$$

where $EC_{50,CA}$ is the prediction value for mixture effects according to the CA model, n is the number of residual micropollutants detected in summer or winter reclaimed water, and pi and $EC_{50,\ I}$ are the fraction and EC_{50} value of micropollutant i in the mixture of detected micropollutants, respectively. The EC_{50} of the targeted micropollutant to *V. fischeri* was obtained from the Quantitative Structure-Activity Relationship, which can be found in our previous study (Ma et al., 2017). The calculated BEQ_{cal} of micropollutant mixtures toward *Vibrio fischeri* was expressed as Eq. 4:

$$BEQ_{cal} = \frac{EC_{50}(phenol)}{EC_{50,CA}/C_{Total}}, \tag{4}$$

where C_{Total} is the overall concentration of the detected micropollutants in the reclaimed water.

3. Results and discussion

3.1. Seasonal and diurnal variations of rDOM

3.1.1. Characteristics of the rDOM

Specific parameters related to photobleaching and photosensitizing of rDOM are organic contents and spectroscopic indices (Niu et al., 2014; Zhang et al., 2019). These relevant properties of rDOM are summarized in Table 1, and published data for comparison are also shown. As expected, seasonal differences were observed; reclaimed water for the experiments was found to have 3.12 mg C/L in summer and 5.43 mg C/L in winter. In the summer, reclaimed water had a lower $SUVA_{254}$, corresponding to lower aromatic contents. Additionally, reclaimed water from the summer had a higher E_2/E_3 value in comparison with the winter season. When E_2/E_3 is between 7.0 and 10.0 (summer reclaimed water, $E_2/E_3 = 8.94$), the vast majority of rDOM are derived from microbially autochthonous organic matter (O'Connor et al., 2019). If E_2/E_3 falls within a range of 5.0–7.0 (winter reclaimed water, $E_2/E_3 = 6.56$), microbial originated autochthonous rDOM and allochthonous DOM both partially account for the reclaimed water. The results indicated that summer rDOM was dominated by autochthonous substances. The summer reclaimed water had higher $S_{275-295}$ and S_R values, indicating that the rDOM molecules were smaller than in the winter. Since autochthonous DOM molecules are smaller than allochthonous DOM molecules (Guerard et al., 2009), the resulting E_2/E_3 values were consistent with $S_{275-295}$ and S_R indexes.

Comparatively, rDOM has different properties than secondary effluent DOM, e.g., rDOM has a significantly lower DOC content and lower molecular weight distribution than secondary effluent DOM. Overall, the summer reclaimed water had smaller rDOM molecules that were dominated by autochthonous substances, while winter reclaimed water had higher aromatic contents with larger rDOM

Table 1
Characters of rDOM and comparisons with WWTP effluents, freshwater isolates.

Parameter	Reclaimed water (this study)		Secondary effluents ($n = 87$)[a]	Freshwater isolates ($n = 2$)[b]
	Summer	Winter	Average	Average
DOC (mg C/L)	3.12	5.43	6.35	10
$SUVA_{254}$ (m^2 g/C)	2.04	2.17	5.24	9.08
E_2/E_3	8.94	6.56	4.97	4.42
$S_{275-295}$ (nm^{-1})	0.0115	0.0074	0.013	0.0129
S_R	0.67	0.46	0.87	0.75
$[^1O_2]ss\ 10^{-13}$ M	0.97	0.83	2.5–11.4	1.2
$[^3DOM^*]ss\ 10^{-14}$ M	0.58	0.44	3.3–46.7	1.8

[a] (O'Connor et al., 2019).
[b] (Wang et al., 2019).

molecules. Although the regular water quality indicators (e.g., COD, nutrients) of summer and winter reclaimed water were similar (Table S3) and met the relevant standards for reuse, the organic components in the reclaimed water were significantly different during different seasons.

Regarding the photosensitizing properties of the rDOM, the steady-state concentrations of three PPRIs (singlet oxygen ($^1O_2$), triplet-excited state of DOM ($^3DOM^*$), and hydroxyl radical (•OH)) were quantified (Text S2) in the irradiated solutions and summarized in Table 1. In the current experiment, the rDOM had a [$^1O_2$]ss range from 0.83×10^{-13} M to 0.93×10^{-13} M, which was lower than that of secondary effluents and freshwater isolates. The reactive transient species are very quickly consumed in sunlit waters; consequentially, aqueous solutions show low steady-state concentrations of PPRIs (typically, 10^{-18}–10^{-12} M) (Vione et al., 2014; Vione and Scozzaro, 2019). When comparing the steady-state concentrations of $^3DOM^*$, the rDOM was shown to be significantly lower than that of secondary effluents and freshwater isolates. As for [•OH]ss, previous studies have concluded that the steady-state concentrations are low, generally approximately 10^{-16} M in the sunlit water, much less than [$^1O_2$]ss and [$^3DOM^*$]ss (Vione and Scozzaro, 2019). This was not observed in this experiment owing to the short irradiation time (10*h*). In addition, the studied rDOM contained many autochthonous fractions that act as a sink of •OH and could lead to a low [•OH]ss (Vione and Scozzaro, 2019). Regarding the DOM components, the higher contents of aromatic carbonyls and quinones, the higher concentration of $^3DOM^*$ after sunlight irradiation (Zhou et al., 2017; Vione and Scozzaro, 2019). Thus, the WWTP effluents with higher aromatic contents may produce higher concentration of active species through photochemical paths. In the present study, the $SUVA_{254}$ of the studied reclaimed water was lower than the WWTP effluents and freshwater (for comparison), which might the reason for the lower observed concentration of active species in the irradiated reclaimed water.

3.1.2. Changes in UV–vis absorbance

As we can see from Fig. 1a1 and b1, sunlight exposure led to a distinctly progressive decrease with time of UV–vis absorbance in summer, while during the winter there was only a slight decrease. The reduction of total CDOM contents was more pronounced for summer reclaimed

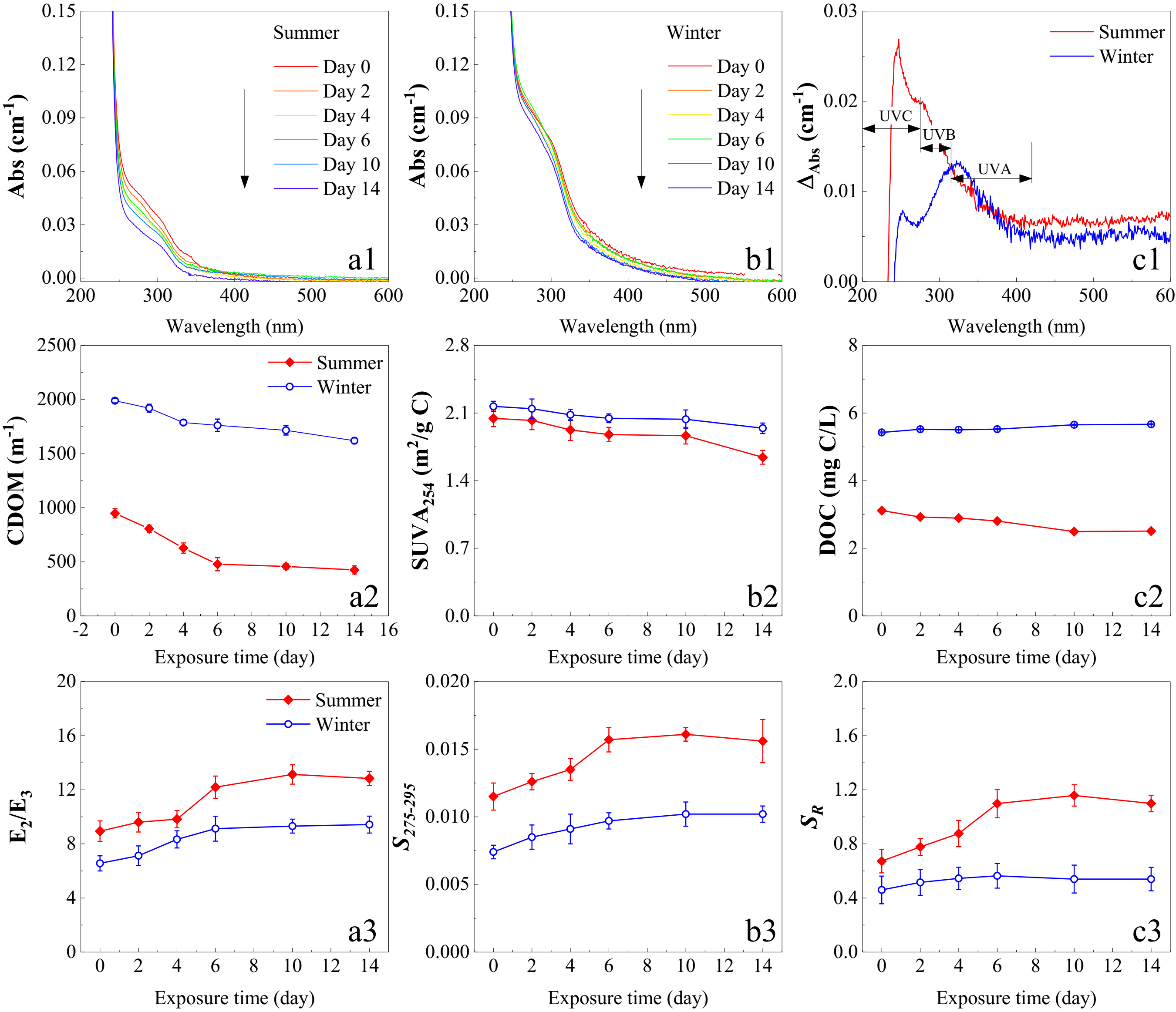

Fig. 1. Changes in the optical indices of rDOM and the DOC contents. Evolution of the absorbance spectra of reclaimed water during solar irradiation in summer (a1) and winter season (b1), decrement (Δ) of absorbance spectra after 14 full-day outdoor tests (c1), CDOM (a2), $SUVA_{254}$ (b2), DOC (c2), E_2/E_3 (a3), $S_{275–295}$ (b3), and S_R (c3).

water than winter reclaimed water: a reduction of 55% and 19% from the initial values, respectively (Fig. 1a2). The degradation of aromatic moieties was also observed, accompanied by the decline in absorption spectra. Specifically, the $SUVA_{254}$ values decreased with removal efficiencies of 20% in summer and 10% in winter after 14 full-day outdoor tests. Along with the photobleaching of rDOM in the storage pond, photomineralization was also observed especially in the summer season (Fig. 1c2), where the DOC of the reclaimed water decreased from 3.12 to 2.44 mg C/L (a 21.8% loss) over a total sunlight exposure of 579.18 kJ/L. DOM molecules can be photomineralized under solar light, and it has been reported that 32%–47% of the DOC may be removed from the DOM pool by natural sunlight in laboratory-scale experiments (Du et al., 2016; Zhou et al., 2018). Yang et al. also found that 45%–59% of the UV-absorbing compounds in WWTP effluents could be eliminated after exposure to sunlight with a total solar irradiance of 5.3×10^5 J/m^2 (Yang et al., 2014). However, the photomineralization of rDOM in winter was negligible during open storage, which could be attributable to lower temperatures and less accumulated solar energy.

As shown in Fig. 1c1, the reduction of UV-absorbing rDOM showed significantly different trends between the summer and winter seasons. The reduction in UV-absorbing rDOM was processed by the preferential removal of chromophores in UVC regions during summer season, while during the winter season preferential removal of chromophores in UVA regions was observed. Although very little UVC reaches the ground after the solar light passes through the atmosphere shell, the results indicated that UVC may govern the changes of UV-absorbing rDOM during the summer season. In addition, it is interesting to note that the changes in E_2/E_3 and S_R values appeared to demonstrate the “Matthew effect” in the process of rDOM photobleaching under field conditions. As the values of E_2/E_3 and S_R are proxies for the degree of photobleaching of rDOM (Helms et al., 2008), the reclaimed water with higher E_2/E_3 and S_R values underwent stronger solar irradiation accompanied by higher temperatures in the summer season. In contrast, the winter reclaimed water with lower E_2/E_3 and S_R values underwent weaker solar irradiation accompanied by lower temperatures (Fig. 1a3 and c3). These conditions led to the rDOM undergoing more pronounced photobleaching in the summer, although the winter rDOM comprised much more CDOM with higher $SUVA_{254}$. This would result in the dissipation of CDOM during summer storage of reclaimed water, while the CDOM in winter reclaimed water would be persistent in the storage pond under sunlight exposure. Besides, continuously increasing E_2/E_3, $S_{275-295}$, and S_R in the summer and winter seasons revealed that there is a shift from high-molecular-weight to low-molecular-weight as rDOM is photobleached (Fig. 1a3, b3, and c3).

3.1.3. Changes in 3DEEM spectra

3DEEM spectra followed by FRI analysis was used to identify and characterize the changes of the FDOM components during each exposure period. As shown in Fig. 2 (S_0 and W_0), there are four identifiable areas in the 3DEEM map of the reclaimed water, which reflect its possible origins and fluorescence information. The 3DEEM maps illustrated that protein-like materials were found to be the main components of summer rDOM, which are attributed to autochthonous production associated with bacteria-derived compounds (Region III). In contrast, winter rDOM was dominated by fulvic and humic acid-like compounds (Regions II and IV) (allochthonous substances). The 3DEEM results confirmed the discrepancies of the aforementioned spectral parameters between the summer and winter reclaimed water.

The total volumetric fluorescence of the reclaimed water was 2.3×10^7 AU·nm^2 for summer and 1.7×10^7 AU·nm^2 for winter. These values were generally similar to values previously reported in WWTP effluents (Chen et al., 2003). Increased sunlight exposure led to notable changes in the 3DEEM spectra, such as Peak R_{II} and Peaks R_{II} and R_{IV}, which appeared to be diminished in rDOM during open-air storage (Fig. 2S_{14} and W_{14}). The photo-induced changes in the level of each fluorescent region were characterized by the volume of fluorescence of corresponding matrixes. As plotted in Fig. S3a, the total volume of fluorescence decreased significantly in both summer and winter. Although higher aromaticity and absorbance were observed for the winter reclaimed water (Table 1), the results showed higher FDOM removal in summer than in winter (49% vs 28%, respectively) after 14 consecutive sunny days. The volumetric fluorescence of the four fluorescent regions decreased with different trends. In the summer season with a total sunlight power of 579.18 kJ/L, the overall reductions of R_I, R_{II}, R_{III}, and R_{IV} were 47%, 52%, 39%, and 60%, respectively. R_{IV} showed the highest attenuation rate, followed by R_{II} (Fig. S3b). In the winter season with a total sunlight power of 204.22 kJ/L, the overall reductions of R_I, R_{II}, R_{III}, and R_{IV} were 8%, 32%,18%, and 45%, respectively. As with the summer reclaimed water, R_{IV} still showed the highest attenuation rate, followed by R_{II} (Fig. S3c). These results strongly suggest that humic acid-like 3DEEM compounds (R_{IV}) derived from wastewater were the most photolabile fractions and were preferentially removed in rDOM during open-air storage regardless of the season.

3.2. Micropollutants attenuation

3.2.1. Occurrence of micropollutants

Overall, 39 out of the 52 targeted organic micropollutants were detected at least once in summer reclaimed water, which contained 3 phenols, 5 OPFRs, 7 sunscreens, 9 pharmaceuticals, 6 bactericides, 8 pesticides, and 1 EDC, while 44 chemicals comprising 3 phenols, 5 OPFRs, 5 sunscreens, 12 pharmaceuticals, 6 bactericides, 9 pesticides, and 4 EDCs were found during the winter season (Table 2). Of the 52 targeted micropollutants, 19 chemicals were always detected ($f = 100\%$), while 7 chemicals (PABA, OD-PABA, αE2, βE2, CYZ, PRT, and TRT) were never detected in the reclaimed water investigated during this study. The highest overall average values were found for DMM (110.3 ng/L), DPH (131.1 ng/L), CBM (143.7), CBZ (162.7 ng/L), BP3 (521.9), ROX (750.6 ng/L), and CLR (861.5 ng/L). Average concentrations of individual micropollutants found in this investigation were consistent with the concentrations found in the effluents of 14 WWTPs by Ben et al. (Ben et al., 2018) and were in line with previously reported concentration ranges for reclaimed water (Ma et al., 2018; Sun et al., 2016). The average concentrations of all residual micropollutants derived from the wastewater were 915.0 ng/L and 3101.8 ng/L in the summer and winter, respectively. Among the seven groups of micropollutants, the main components found in the reclaimed water in the summer and winter seasons were pharmaceuticals (35% and 62% of the total concentrations, respectively) and sunscreens (20% and 17% of the total concentrations, respectively). The acquired reclaimed water was mainly derived from municipal wastewater, and thus the residual micropollutants in the wastewater were closely related to the productive activities of human beings as well as sewage treatment techniques (Besha et al., 2017; Grandclement et al., 2017). The detected pharmaceuticals and sunscreens that dominated in the reclaimed water all belonged to pharmaceutical and personal care products (PPCPs), which was a category of pseudo-persistent pollutant due to their incomplete removal and continuous discharge (Grandclement et al., 2017).

The total concentrations of residual micropollutants were much higher in winter than in summer (3101.8 and 915.0 ng/L, respectively). Similar results were seen in the pharmaceuticals (1908.6 ng/L in the winter and 323.6 ng/L in the summer) and sunscreens (533.6 ng/L in the winter and 178.6 ng/L in the summer). Seasonal variations in the remaining concentration of PPCPs in effluent waters were also observed by Vieno et al. (Vieno et al., 2005), who found that the total concentration of all studied PPCPs was 3–5 times higher in the winter than during other seasons. In the present study, the discrepancies in seasonal concentrations for micropollutants may be attributed to the lower temperatures during the winter season (Grandclement et al., 2017).

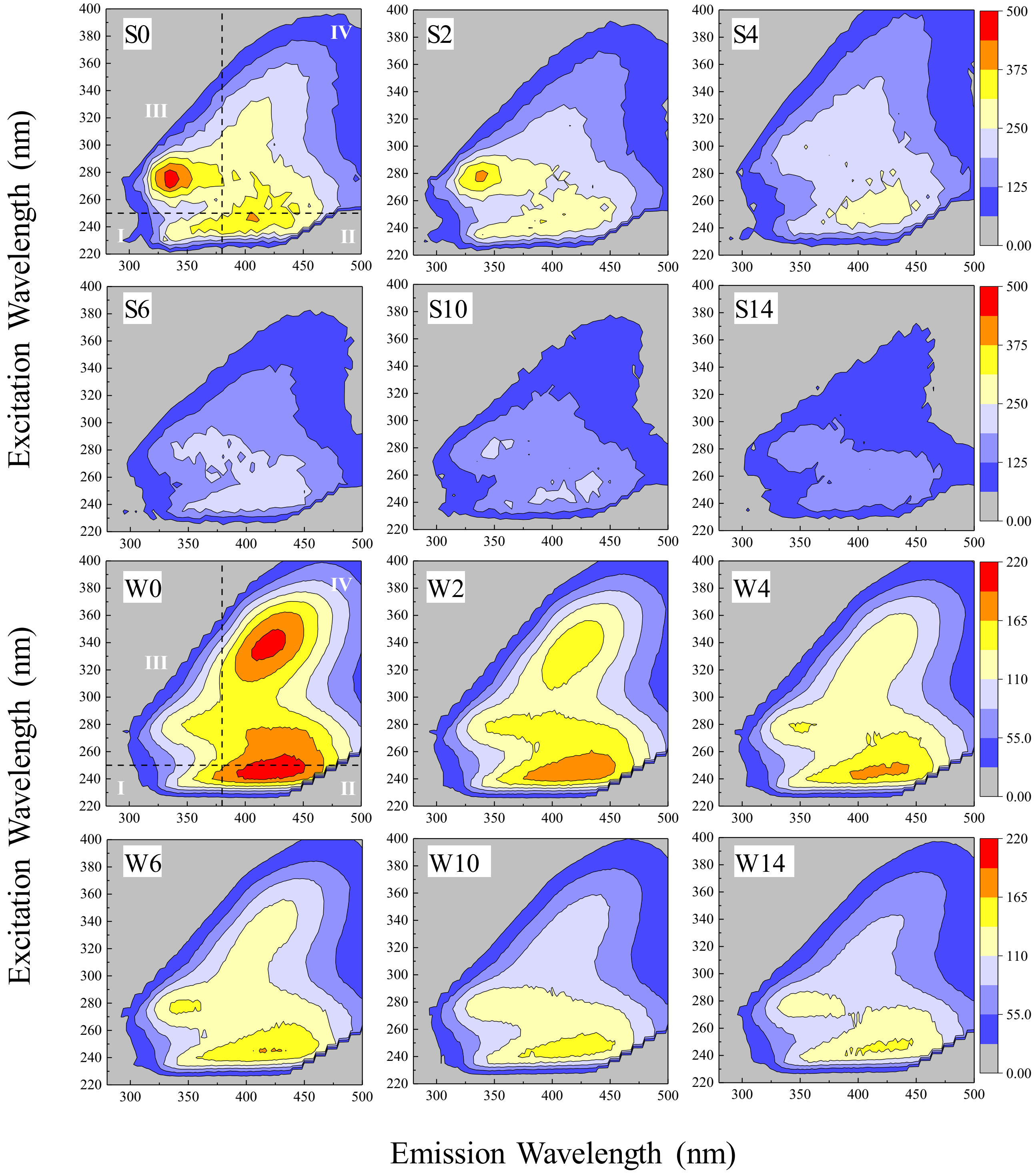

Fig. 2. 3DEEM spectra diagrams of the initial and photo-exposed rDOM during summer and winter season. Si (i = 0, 2, 4, 6, 10, 14 days) represents the summer reclaimed water under sunlight exposure, while the Wi (*i* = 0, 2, 4, 6, 10, 14 days) represents the winter reclaimed water under sunlight exposure.

3.2.2. Attenuation behavior of micropollutants

Fig. S4 summarizes the attenuation behaviors of the residual micropollutants in the open-air storage ponds. The attenuation of micropollutants improved along with sunlight exposure time in both the summer and winter seasons. Over a total sunlight exposure of 579.18 kJ/L, the concentration of total micropollutants gradually attenuated from 1075 ng/L to 369 ng/L with 66% removal efficiency in the summer exposure period, while the concentration of total micropollutants declined from 2803 ng/L to 2124 ng/L with 24% removal efficiency in the winter exposure period (a total sunlight exposure of 204.22 kJ/L). Among the seven groups of micropollutants, EDCs, sunscreens, and pharmaceuticals were effectively eliminated (>75% removal) after summer exposure, while the efficiency of pesticide, bactericide, OPFR, and phenol removals were 46%, 48%, 29%, and 22%, respectively. All seven groups of micropollutants showed poor attenuation (<30% removal) during the winter season except for phenols (60% removal).

The removal of individual micropollutants could be roughly categorized as highly removed (>85% removal), easily removed (60%–85%

Table 2
Frequency (f) of detection, mean concentration (Conc.) and standard deviations of 52 micropollutants in the reclaimed water during summer and winter season.

Group	Chemical	Abbr.	Summer		Winter	
			f (%)	Conc. (ng/L)	*f* (%)	Conc. (ng/L)
Pharmaceuticals	Naproxen	NPX	–	–	75%	6.1 ± 4.2
	Mefenamic acid	MEF	–	–	25%	1.8 ± 3.1
	Ibuprofen	IBU	50%	9.7 ± 15.0	100%	37.6 ± 38.3
	Roxithromycin	ROX	100%	88.1 ± 39.3	100%	750.6 ± 317.3
	Sulfamethoxazole	SMX	25%	5.2 ± 9.0	100%	15.3 ± 11.3
	Trimethoprim	TMT	–	–	100%	32.0 ± 37.1
	Clarithromycin	CLR	75%	14.6 ± 9.6	100%	861.5 ± 190.5
	Erythromycin	ERY	50%	8.5 ± 13.2	100%	8.9 ± 4.0
	Ketoprofen	KPF	50%	2.4 ± 3.8	100%	3.5 ± 1.7
	Carbamazepine	CBZ	100%	162.7 ± 57.9	100%	56.5 ± 23.7
	Diphenhydramine Hydrochloride	DPH	100%	32.2 ± 28.4	100%	131.1 ± 62.2
	Fluoxetine hydrochloride	FLX	25%	0.2 ± 0.3	100%	3.8 ± 1.8
	Total pharmaceuticals			323.6 ± 56.5		1908.6 ± 367.0
Sunscreens	Benzophenone-1	BP1	50%	3.1 ± 3.1	100%	8.0 ± 5.2
	Oxybenzone	BP3	75%	23.4 ± 23.9	100%	521.9 ± 83.5
	2-Benzoyl-5-methoxy-1-phenol-4-sulfonic acid	BP4	100%	2.6 ± 2.3	25%	1.2 ± 2.0
	4-Aminobenzoic acid	PABA	–	–	–	–
	Octocrilene	OC	100%	65.1 ± 12.4	50%	0.4 ± 0.5
	2-Ethylhexyl 4-dimethylaminobenzoat	OD-PABA	–	–	–	–
	Avobenzone	BM-DBM	100%	7.3 ± 3.8	–	–
	Octyl 4-methoxycinnamat	EHMC	100%	77.2 ± 7.4	100%	2.2 ± 2.1
	Total sunscreens			178.6 ± 20.0		533.6 ± 78.9
EDCs	Estrone	E1	–	–	100%	0.3 ± 0.2
	Estriol	E3	–	–	100%	0.3 ± 0.1
	17-alpha-Estradiol	α E2	–	–	–	–
	17-beta-Estradiol	β E2	–	–	–	–
	17a-Ethinylestradiol	EE2	–	–	25%	0.1 ± 0.1
	Bisphenol A	BPA	100%	89.8 ± 10.2	100%	37.7 ± 9.3
	Total EDCs			89.8 ± 10.2		38.4 ± 9.2
Pesticides	Simazine	SMZ	50%	0.7 ± 0.8	100%	5.3 ± 3.0
	Atrazine	Atrazine	100%	1.4 ± 0.2	100%	2.9 ± 1.0
	Cyanazine	CYZ	–	–	–	–
	Prometryne	PRT	–	–	–	–
	Ametryn	Ametryn	75%	0.3 ± 0.2	100%	0.2 ± 0.0
	Terbuthylazine	TET	50%	0.1 ± 0.1	100%	1.3 ± 0.2
	Dichlorvos	DDVP	25%	1.2 ± 2.0	100%	10.3 ± 2.7
	Triallate	TRT	–	–	–	–
	Trichlorfon	TRF	–	–	100%	0.8 ± 0.3
	Acetamiprid	ACT	100%	17.6 ± 2.5	100%	0.7 ± 0.2
	Imidacloprid	IMP	100%	15.5 ± 6.8	100%	1.7 ± 0.6
	Thiamethoxam	Thixam	100%	17.3 ± 2.7	100%	2.3 ± 1.3
	Total pesticides			54.0 ± 9.7		25.6 ± 3.0
Bactericides	Carbendazim	CBM	100%	39.2 ± 18.4	100%	143.7 ± 102.7
	Prochloraz	PCL	75%	1.8 ± 3.0	100%	4.4 ± 1.7
	Azoxystrobin	Azobin	100%	26.7 ± 23.9	100%	20.8 ± 8.8
	Dimethomorph	DMM	100%	28.6 ± 11.5	100%	110.3 ± 76.9
	Difenoconazole	DFZ	100%	6.7 ± 2.7	100%	6.5 ± 4.0
	Triadimefon	TAN	75%	3.8 ± 3.0	100%	6.0 ± 1.2
	Total bactericides			106.9 ± 37.6		291.8 ± 60.1
OPFRs	Tris(2-Chloroethyl) phosphate	TCEP	100%	49.7 ± 19.0	100%	41.4 ± 11.1
	Triphenyl phosphate	TPhP	50%	3.0 ± 4.8	100%	12.1 ± 3.5
	Triphenylphosphine oxide	TPPO	100%	5.4 ± 3.3	100%	33.9 ± 17.5
	Tributyl phosphate	TBP	100%	6.5 ± 4.7	100%	25.5 ± 9.9
	Tris(1-chloro-2-propyl) phosphate	TCPP	75%	9.2 ± 8.4	100%	83.2 ± 7.8
	Total OPFRs			73.9 ± 20.7		196.1 ± 45.5
Phenols	Phenol	Phenol	100%	38.5 ± 14.8	100%	65.7 ± 8.8
	p-Cresol	p-Cresol	100%	41.6 ± 16.1	100%	33.8 ± 11.3
	2,4,6-Trichlorophenol	2,4,6-TCP	100%	8.1 ± 4.2	100%	8.2 ± 1.2
	Total phenols			88.3 ± 11.9		107.7 ± 18.9
Total micropollutants				915.0 ± 130.3		3101.8 ± 438.9

removal), moderately removed (40%–60% removal), or difficult to remove (<40% removal). During the summer exposure period, 27 out of 34 residual micropollutants in reclaimed water were eliminated with more than 40% removal (Fig. 3). Notably, there were 10 chemicals in summer reclaimed water, including SMX, Ametryn, TBZ, IMP, IBU, ERY, KPF, BP1, BP4, and BM-DBM, which were highly removed and not detected in the open-air storage ponds after 14 full sunny days of exposure. During the winter exposure period, 31 out of 42 residual micropollutants in reclaimed water were eliminated with less than 40% removal. There were only 3 chemicals (E2, Ametryn, and KPF) that were highly removed and not detected in the open-air storage ponds after 14 full sunny days of exposure.

Thanks to the sunlight irradiation, the residual micropollutants with environmentally realistic concentrations showed remarkable attenuation in the open-air storage ponds during the summer season. Photosensitive micropollutants such as BP1, IMP, KPF, and SMX underwent direct photolysis (Baena-Nogueras et al., 2017; Paredes et al., 2018). These micropollutants showed a high reduction in the studied reclaimed water during open-air storage. The residual micropollutants could also be degraded by indirect photolysis through the reaction

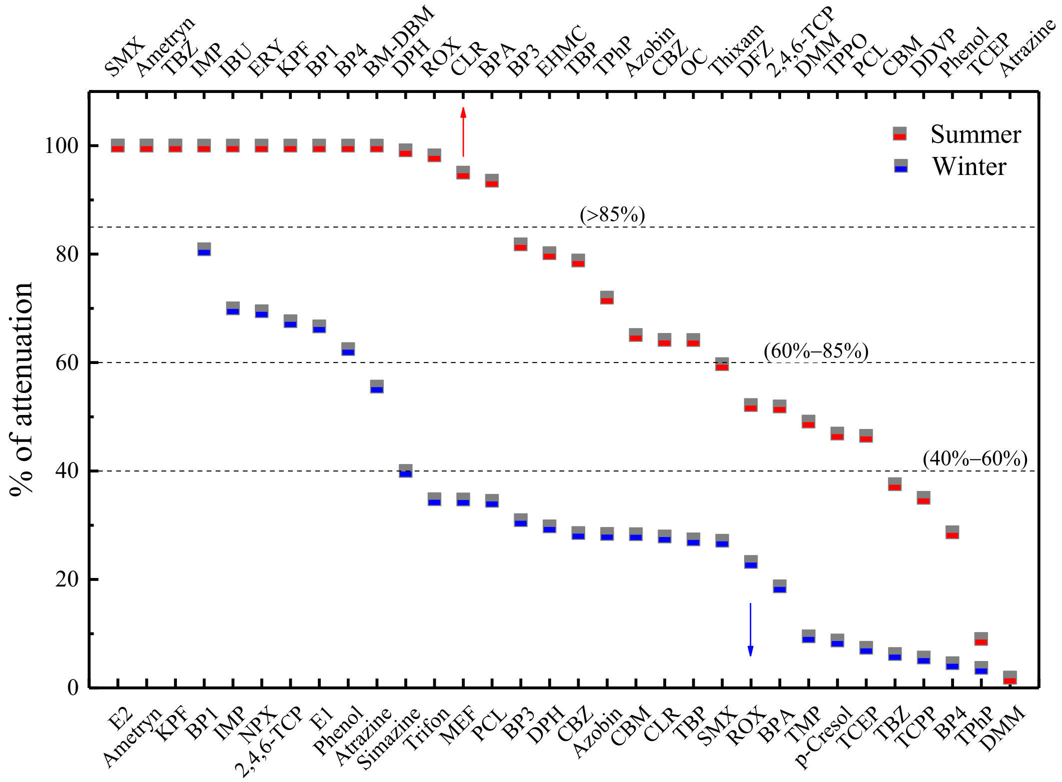

Fig. 3. Percentage attenuation of individual micropollutants in the open-air storage ponds of reclaimed water. Percentage attenuation of individual micropollutants that less than 0 were not shown.

with PPRIs formed by the sunlight excitation of photosensitizers. Among the studied micropollutants, ERY, DPH, ROX, CLR, BP1, OC, and BP3 were all defined as direct photo-stable chemicals (Baena-Nogueras et al., 2017; Batchu et al., 2014; López et al., 2017), but effective elimination with high removal rates (>80%) was achieved after natural sunlight exposure, which can likely be ascribed to indirect photolysis. The chemical of CBZ remaining in the reclaimed water is difficult to remove in a variety of treatment processes (Matamoros et al., 2008a; Matamoros et al., 2008b), but significant removal (59%) was observed in the storage pond after summer exposure. The attenuation of CBZ may be attributed to the HO•, which has been reported to be the only transient reactive species to effectively degrade CBZ in sunlit waters (Vione and Scozzaro, 2019). Although the photolysis mechanism of micropollutants in the actual reclaimed water was complicated and influenced by many factors, such as sunlight irradiation, water depth, organic matter concentration, pH, and temperature (Bora and Mewada, 2017), the results revealed that substantial attenuation of micropollutants was observed during the open storage of reclaimed water in the summer season, while natural sunlight showed negligible effects on micropollutants in the winter season.

3.3. Toxicity evolution

3.3.1. Reduction of acute toxicity

The luminescent bacteria assay showed that the average acute toxicity of the summer reclaimed water was 14.4 mg/L BEQ_{phenol}, while that of the winter reclaimed water was 14.1 mg/L BEQ_{phenol}. The luminescent bacteria toxicity test is a nonspecific assay, which can react to most chemicals including known and unknown mixtures (Tang et al., 2014). Previous studies have reported that BEQ_{phenol} of the WWTP effluent ranged from 5.0 to 20 mg/L (Jia et al., 2015; Ma et al., 2019), which is consistent with the present study. Fig. 4 shows the luminescent bacteria acute toxicity evolution during sunlight exposure of the reclaimed water mixtures in the summer and winter seasons. Specifically, the acute toxicity posed by the reclaimed water decreased from 14.4 mg/L to 1.9 mg/L in summer, while the acute toxicity in the winter reclaimed water decreased from 14.1 mg/L to 9.1 mg/L after 14 full days of sunlight exposure. It was observed that not only did the attenuation of macromolecular rDOM and micromolecular micropollutants take place, but the mitigation of acute toxicity from reclaimed water also occurred during open-air storage owing to the sunlight irradiation. Du et al. indicated that natural sunlight could reduce the cytotoxicity of sewage effluents to CHO cells (a Chinese hamster ovary cell line) and that direct photolysis was the main contributor to the toxicity reduction, while the generated PPRIs also contributed to the reduction of cytotoxicity (Du et al., 2018a, 2018b; Lv et al., 2017). The present study confirmed that natural

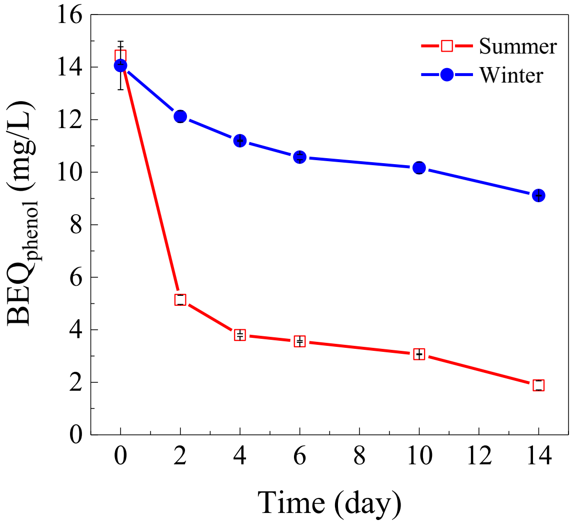

Fig. 4. The luminescent bacteria acute toxicity evolution during sunlight exposure of the reclaimed water in the open-air storage pond.

sunlight played a significant role in the detoxification of reclaimed water during open storage and was indeed a natural purification process.

3.3.2. Correlation between acute toxicity and residual organics in reclaimed water

The experimental BEQ_{bio} of reclaimed water mixtures was responsible for all SPE extracts, which are a "cocktail" of organic matter containing macromolecular rDOM and micromolecular micropollutants. As shown in Fig. 5, the luminescent bacteria acute toxicity caused by the detected micropollutants could only explain 0.02%–2% of acute toxicity from the reclaimed water mixtures during the summer and winter seasons. The results indicated that the variation of cytotoxicity of reclaimed water mixtures (BEQ_{bio}) could not be well predicted using the calculated BEQ_{cal}, which was derived from the detected micropollutants. It has been reported the detected chemicals explained less than 3% of luminescent bacteria acute toxicity even when a total of 299 chemicals were screened (Tang et al., 2014). Hence, the deviation between the experimental and calculated acute toxicity may result from "unknown mixtures," such as bulk rDOM, which were responsible for the bioluminescence inhibition effect.

To better understand the relationship between BEQ_{bio} reduction and rDOM or micropollutants during natural sunlight exposure, RDA was conducted based on the dataset obtained from the field experiments. The dependent variables were BEQ_{bio} and BEQ_{cal} (used as a comparison), and the independent variables included in the model were micropollutants (total concentrations), DOC, CDOM, $SUVA_{254}$, E_2/E_3, S_R, and FDOM. Fig. 6 shows the superimposed RDA biplots of organic parameters and acute toxicity during the summer and winter experimental periods. When the angle of the vectors is less than 90°, a positive correlation is expected; when they point in opposite directions, the expected correlation is negative. During the summer exposure period, the statistical analysis elucidated that a positive correlation existed between BEQ_{bio} and FDOM, CDOM, DOC, $SUVA_{254}$, and micropollutants (Fig. 6a). The fact that the angle between BEQ_{bio} and FDOM and CDOM was smaller than other parameters indicated that FDOM and CDOM were more important than other independent variables in the reduction of $BEQ_{bio.}$ In particular, the winter season showed substantial reduction of acute toxicity, while negligible photomineralization of DOC and low attenuation of micropollutants were observed during open storage of reclaimed water. The RDA analysis showed that a significant correlation was found between the variations of BEQ_{bio} and FDOM and CDOM (Fig. 6b), while BEQ_{cal} only showed a positive correlation with the variations of micropollutant concentration. This indicated that the photobleaching or conformational changes of the FDOM and CDOM under natural sunlight irradiation seemed to control the reduction of acute toxicity in the open-air storage pond. A negative correlation was found between BEQ_{bio} and E_2/E_3, S_R whether in summer or winter, verifying that a shift from high-molecular-weight to low-molecular-weight as rDOM is photobleached was beneficial for the reduction of acute toxicity during reclaimed water open-air storage. Lv et al. reported that the cytotoxicity of high-molecular-weight fractions (>1 kDa) was undetectable after 6 h of simulated solar light irradiation, which is consistent with the present study (Lv et al., 2017). Based on the results, it is possible to deduce that macromolecular rDOM is critical to the reduction of acute toxicity, and that the sunlight-induced changes in FDOM and CDOM were significantly correlated with the reduction of acute toxicity during open-air storage of reclaimed water.

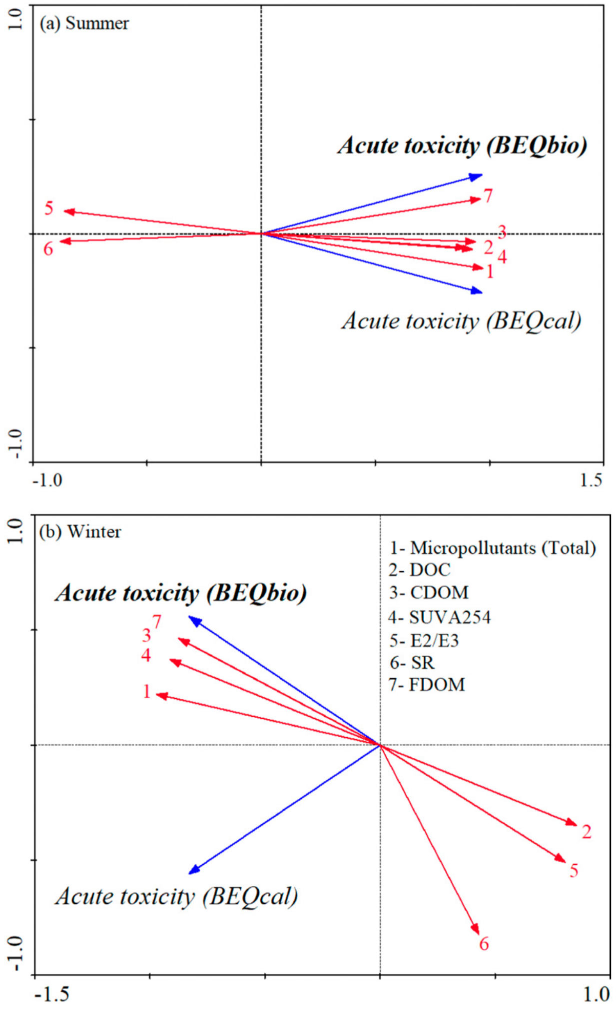

Fig. 6. Ordination diagrams for the Redundancy analysis (RDA): (a) superimposed RDA biplots of organic parameters and acute toxicity during summer exposure period; (b) superimposed RDA biplots of organic parameters and acute toxicity during winter exposure period. Quantitative independent variables are represented by red arrows, while dependent variables are represented by blue arrows. (For interpretation of the references to colour in this figure legend, the reader is referred to the web version of this article.)

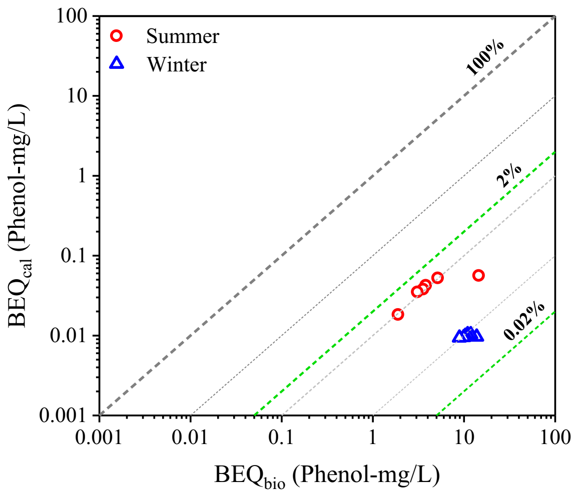

Fig. 5. Contribution of detected chemicals to the acute toxicity toward *Vibrio fischeri* during summer and winter exposure period. BEQ_{cal} represents the calculated acute toxicity of reclaimed water from the detected micropollutants, while BEQ_{bio} represents the acute toxicity of reclaimed water from the bioluminescence inhibition assay.

4. Conclusion

Seasonal and long-term open storage of reclaimed water is often required to equalize production and demand in water supply systems. In the present study, when the reclaimed water was stored in an open-air pond decontamination and detoxification were observed after 14 consecutive sunny days in both the summer and winter seasons. During sunlight exposure in the open storage pond, significant photobleaching and the generation of PPRIs including $^1O_2$ and $^3DOM^*$ were observed in reclaimed water. However, sunlight-induced changes in CDOM absorption and FDOM components showed different characteristics between the summer and winter seasons. Specifically, CDOM absorption in UVC regions was preferentially removed in the summer, while tests in the winter season showed preferential removal of CDOM in UVA regions. Tests in both seasons showed that the attenuation in FDOM was more pronounced for allochthonous substances than autochthonous substances. Regarding the residual micropollutants in reclaimed water during open storage, the total concentration of 52 targeted chemicals achieved 66% attenuation in summer and only 24% in winter. Among the seven groups of micropollutants, EDCs, sunscreens, and pharmaceuticals were effectively eliminated (>75% removal) in the summer season. Moreover, sunlight exposure significantly lowered the luminescent bacteria acute toxicity of reclaimed water during summer and winter storage. The comprehensive mathematical calculation combined with RDA analysis revealed that sunlight-induced changes in FDOM and CDOM may be principally responsible for the detoxification process. Further studies are still necessary in order to investigate how certain residual organic components in reclaimed water affect the reduction of biotoxicity under sunlight irradiation.

CRediT authorship contribution statement

Yongkun K. Wang: Writing- Original draft preparation, Formal analysis. Xiaoyan Y. Ma: Writing - Review & Editing, Supervision. Shiying Zhang: Methodology, Investigation. Lei Tang: Data Curation. Hengfeng Zhang: Methodology, Data. Xiaochang C. Wang: Writing - Review & Editing, Supervision.

Declaration of competing interest

The authors declare that they have no known competing financial interests or personal relationships that could have appeared to influence the work reported in this paper.

Acknowledgements

This study was supported by the National Natural Science Foundation of China (Grant No. 51778522), and Natural Science Foundation of Shaanxi Province (No. 2020JQ-663).

Appendix A. Supplementary data

Supplementary data to this article can be found online at https://doi.org/10.1016/j.scitotenv.2020.141768.

References

Baena-Nogueras, R.M., Gonzalez-Mazo, E., Lara-Martin, P.A., 2017. Degradation kinetigehcs of pharmaceuticals and personal care products in surface waters: photolysis vs biodegradation. Sci. Total Environ. 590-591, 643–654.

Bahnmuller, S., von Gunten, U., Canonica, S., 2014. Sunlight-induced transformation of sulfadiazine and sulfamethoxazole in surface waters and wastewater effluents. Water Res. 57, 183–192.

Batchu, S.R., Panditi, V.R., O'Shea, K.E., Gardinali, P.R., 2014. Photodegradation of antibiotics under simulated solar radiation: implications for their environmental fate. Sci. Total Environ. 470-471, 299–310.

Ben, W., Zhu, B., Yuan, X., Zhang, Y., Yang, M., Qiang, Z., 2018. Occurrence, removal and risk of organic micropollutants in wastewater treatment plants across China: comparison of wastewater treatment processes. Water Res. 130, 38–46.

Besha, A.T., Gebreyohannes, A.Y., Tufa, R.A., Bekele, D.N., Curcio, E., Giorno, L., 2017. Removal of emerging micropollutants by activated sludge process and membrane bioreactors and the effects of micropollutants on membrane fouling: a review. Journal of Environmental Chemical Engineering 5 (3), 2395–2414.

Bodhipaksha, L.C., Sharpless, C.M., Chin, Y.P., MacKay, A.A., 2017. Role of effluent organic matter in the photochemical degradation of compounds of wastewater origin. Water Res. 110, 170–179.

Bora, L.V., Mewada, R.K., 2017. Visible/solar light active photocatalysts for organic effluent treatment: fundamentals, mechanisms and parametric review. Renew. Sust. Energ. Rev. 76, 1393–1421.

Chen, W., Westerhoff, P., Leenheer, J.A., Booksh, K., 2003. Fluorescence excitation-emission matrix regional integration to quantify spectra for dissolved organic matter. Environ. Sci. Technol. 37 (24), 5701–5710.

Cirelli, G.L., Consoli, S., Di Grande, V., 2008. Long-term storage of reclaimed water: the case studies in Sicily (Italy). Desalination 218 (1–3), 62–73.

Du, Y., Wu, Q.Y., Lv, X.T., Wang, Q.P., Lu, Y., Hu, H.Y., 2018a. Exposure to solar light reduces cytotoxicity of sewage effluents to mammalian cells: roles of reactive oxygen and nitrogen species. Water Res. 143, 570–578.

Du, Y., Wu, Q.Y., Lv, X.T., Ye, B., Zhan, X.M., Lu, Y., Hu, H.Y., 2018b. Electron donating capacity reduction of dissolved organic matter by solar irradiation reduces the cytotoxicity formation potential during wastewater chlorination. Water Res. 145, 94–102.

Du, Y., Zhang, Y., Chen, F., Chang, Y., Liu, Z., 2016. Photochemical reactivities of dissolved organic matter (DOM) in a sub-alpine lake revealed by EEM-PARAFAC: an insight into the fate of allochthonous DOM in alpine lakes affected by climate change. Sci. Total Environ. 568, 216–225.

Du, Y., Zhang, X., Li, C., Wu, Q.Y., Huang, H., Hu, H.Y., 2017. Transformation of DON in reclaimed water under solar light irradiation leads to decreased haloacetamide formation potential during chloramination. J. Hazard. Mater. 340, 319–325.

Ge, J., Huang, D., Han, Z., Wang, X., Wang, X., Wang, Z., 2019. Photochemical behavior of benzophenone sunscreens induced by nitrate in aquatic environments. Water Res. 153, 178–186.

Giannakis, S., Polo López, M.I., Spuhler, D., Sánchez Pérez, J.A., Fernández Ibáñez, P., Pulgarin, C., 2016. Solar disinfection is an augmentable, in situ -generated photo-Fenton reaction—part 1: a review of the mechanisms and the fundamental aspects of the process. Appl. Catal. B Environ. 199, 199–223.

Grandclement, C., Seyssiecq, I., Piram, A., Wong-Wah-Chung, P., Vanot, G., Tiliacos, N., Roche, N., Doumenq, P., 2017. From the conventional biological wastewater treatment to hybrid processes, the evaluation of organic micropollutant removal: a review. Water Res. 111, 297–317.

Guerard, J.J., Miller, P.L., Trouts, T.D., Chin, Y.P., 2009. The role of fulvic acid composition in the photosensitized degradation of aquatic contaminants. Aquat. Sci. 71 (2), 160–169.

Hawker, D.W., Cumming, J.L., Neale, P.A., Bartkow, M.E., Escher, B.I., 2011. A screening level fate model of organic contaminants from advanced water treatment in a potable water supply reservoir. Water Res. 45 (2), 768–780.

Helms, J.R., Stubbins, A., Ritchie, J.D., Minor, E.C., Kieber, D.J., Mopper, K., 2008. Absorption spectral slopes and slope ratios as indicators of molecular weight, source, and photobleaching of chromophoric dissolved organic matter. Limnol. Oceanogr. 53 (3), 955–969.

Hu, H., Du, Y., Wu, Q., Chen, Z., Yang, H., Lu, Y., Li, K., 2018. Building the security guarantee system for water potable reuse in the vision of systematic engineering. Res. Environ. Sci. 31, 1163–1173.

Hu, H.Y., Du, Y., Wu, Q.Y., Zhao, X., Tang, X., Chen, Z., 2016. Differences in dissolved organic matter between reclaimed water source and drinking water source. Sci. Total Environ. 551-552, 133–142.

Hu, Y., Yang, Y., Wang, X.C., Hao Ngo, H., Sun, Q., Li, S., Tang, J., Yu, Z., 2017. Effects of powdered activated carbon addition on filtration performance and dynamic membrane layer properties in a hybrid DMBR process. Chem. Eng. J. 327, 39–50.

ISO 11348, 2008. Water quality - determination of the inhibitory effect of water samples on the light19 emission of Vibrio fischeri (luminescent bacteria test). Eur. Norm.

Jasper, J.T., Sedlak, D.L., 2013. Phototransformation of wastewater-derived trace organic contaminants in open-water unit process treatment wetlands. Environ. Sci. Technol. 47 (19), 10781–10790.

Jia, A., Escher, B.I., Leusch, F.D.L., Tang, J.Y.M., Prochazka, E., Dong, B., Snyder, E.M., Snyder, S.A., 2015. In vitro bioassays to evaluate complex chemical mixtures in recycled water. Water Res. 80, 1–11.

López, N., Plaza, S., Afkhami, A., Marco, P., Giménez, J., Esplugas, S., 2017. Treatment of diphenhydramine with different AOPs including photo-Fenton at circumneutral pH. Chem. Eng. J. 318, 112–120.

Lv, X.T., Zhang, X., Du, Y., Wu, Q.Y., Lu, Y., Hu, H.Y., 2017. Solar light irradiation significantly reduced cytotoxicity and disinfection byproducts in chlorinated reclaimed water. Water Res. 125, 162–169.

Lyu, S., Chen, W., Zhang, W., Fan, Y., Jiao, W., 2016. Wastewater reclamation and reuse in China: opportunities and challenges. J. Environ. Sci. 39, 86–96.

Ma, X., Wang, X., Liu, Y., Gao, J., Wang, Y., 2017. Variations in toxicity of semi-coking wastewater treatment processes and their toxicity prediction. Ecotoxicol. Environ. Saf. 138, 163–169.

Ma, X.Y., Wang, X.C., Wang, D., Ngo, H.H., Zhang, Q., Wang, Y., Dai, D., 2016. Function of a landscape lake in the reduction of biotoxicity related to trace organic chemicals from reclaimed water. J. Hazard. Mater. 318, 663–670.

Ma, X.Y., Li, Q., Wang, X.C., Wang, Y., Wang, D., Huu Hao, N., 2018. Micropollutants removal and health risk reduction in a water reclamation and ecological reuse system. Water Res. 138, 272–281.

Ma, X.Y., Wang, Y., Dong, K., Wang, X.C., Zheng, K., Hao, L., Huu Hao, N., 2019. The treatability of trace organic pollutants in WWTP effluent and associated biotoxicity reduction by advanced treatment processes for effluent quality improvement. Water Res. 159, 423–433.

Matamoros, V., Caselles-Osorio, A., Garcia, J., Bayona, J.M., 2008a. Behaviour of pharmaceutical products and biodegradation intermediates in horizontal subsurface flow constructed wetland. A microcosm experiment. Sci. Total Environ. 394 (1), 171–176.

Matamoros, V., Duhec, A., Albaigés, J., Bayona, J.M., 2008b. Photodegradation of carbamazepine, ibuprofen, ketoprofen and 17α-ethinylestradiol in fresh and seawater. Water Air Soil Pollut. 196 (1), 161.

Michael-Kordatou, I., Michael, C., Duan, X., He, X., Dionysiou, D.D., Mills, M.A., Fatta-Kassinos, D., 2015. Dissolved effluent organic matter: characteristics and potential implications in wastewater treatment and reuse applications. Water Res. 77, 213–248.

Miller, G., Quinlan, E., 2003. Impact of Surface Storage on Reclaimed Water: Seasonal and Long Term. Iwa Publishing.

Niu, X.Z., Liu, C., Gutierrez, L., Croue, J.P., 2014. Photobleaching-induced changes in photosensitizing properties of dissolved organic matter. Water Res. 66, 140–148.

O'Connor, M., Helal, S.R., Latch, D.E., Arnold, W.A., 2019. Quantifying photo-production of triplet excited states and singlet oxygen from effluent organic matter. Water Res. 156, 23–33.

Paredes, L., Omil, F., Lema, J.M., Carballa, M., 2018. What happens with organic micropollutants during UV disinfection in WWTPs? A global perspective from laboratory to full-scale. J. Hazard. Mater. 342, 670–678.

Pereira, André M.P.T., Silva, L.J.G., Laranjeiro, Célia S.M., Meisel, L.M., Lino, C.M., Pena, A., 2017. Human pharmaceuticals in portuguese rivers: the impact of water scarcity in the environmental risk. Sci. Total Environ. 609, 1182–1191.

Sardana, A., Cottrell, B., Soulsby, D., Aziz, T.N., 2019. Dissolved organic matter processing and photoreactivity in a wastewater treatment constructed wetland. Sci. Total Environ. 648, 923–934.

Shannon, M.A., Bohn, P.W., Elimelech, M., Georgiadis, J.G., Marinas, B.J., Mayes, A.M., 2008. Science and technology for water purification in the coming decades. Nature 452 (7185), 301–310.

Song, K., Shang, Y., Wen, Z., Jacinthe, P.A., Liu, G., Lyu, L., Fang, C., 2019. Characterization of CDOM in saline and freshwater lakes across China using spectroscopic analysis. Water Res. 150, 403–417.

Sun, J., Ji, X., Zhang, R., Huang, Y., Liang, Y., Du, J., Xie, X., Li, A., 2016. Endocrine disrupting compounds reduction and water quality improvement in reclaimed municipal wastewater: a field-scale study along Jialu River in north China. Chemosphere 157, 232–240.

Tang, J.Y.M., McCarty, S., Glenn, E., Neale, P.A., Warne, M.S.J., Escher, B.I., 2013. Mixture effects of organic micropollutants present in water: towards the development of effect-based water quality trigger values for baseline toxicity. Water Res. 47 (10), 3300–3314.

Tang, J.Y.M., Busetti, F., Charrois, J.W.A., Escher, B.I., 2014. Which chemicals drive biological effects in wastewater and recycled water? Water Res. 60, 289–299.

United Nations Environment Programme, E.E.A.P, 2016. Environmental effects of ozone depletion and its interactions with climate change: progress report, 2015. Photochem. Photobiol. Sci. 15 (2), 141–174.

Vieno, N.M., Tuhkanen, T., Kronberg, L., 2005. Seasonal variation in the occurrence of pharmaceuticals in effluents from a sewage treatment plant and in the recipient water. Environ. Sci. Technol. 39 (21), 8220–8226.

Vione, D., Scozzaro, A., 2019. Photochemistry of surface fresh waters in the framework of climate change. Environ. Sci. Technol. 53, 7945–7963.

Vione, D., Minella, M., Maurino, V., Minero, C., 2014. Indirect photochemistry in sunlit surface waters: photoinduced production of reactive transient species. Chemistry 20, 10590–10606.

Wang, J., Chen, J., Qiao, X., Zhang, Y.N., Uddin, M., Guo, Z., 2019. Disparate effects of DOM extracted from coastal seawaters and freshwaters on photodegradation of 2,4-dihydroxybenzophenone. Water Res. 151, 280–287.

Wang, X.-H., Lin, A.Y.-C., 2014. Is the phototransformation of pharmaceuticals a natural purification process that decreases ecological and human health risks? Environ. Pollut. 186, 203–215.

Wang, Y., Roddick, F.A., Fan, L., 2017. Direct and indirect photolysis of seven micropollutants in secondary effluent from a wastewater lagoon. Chemosphere 185, 297–308.

Wu, Qian-Yuan, Chao, L., Ye, D., Wen-Long, W., Huang, H., Hong-Ying, H., 2016a. Elimination of disinfection byproduct formation potential in reclaimed water during solar light irradiation. Water Res. 95, 260–267.

Wu, Q., Li, C., Wang, W., He, T., Hu, H., Du, Y., Wang, T., 2016b. Removal of fluorescence and ultraviolet absorbance of dissolved organic matter in reclaimed water by solar light. J. Environ. Sci. 43, 118–127.

Yang, X., Meng, F., Huang, G., Sun, L., Lin, Z., 2014. Sunlight-induced changes in chromophores and fluorophores of wastewater-derived organic matter in receiving waters—the role of salinity. Water Res. 62, 281–292.

Zhang, X., Yang, C.W., Li, J., Yuan, L., Sheng, G.P., 2019. Spectroscopic insights into photochemical transformation of effluent organic matter from biological wastewater treatment plants. Sci. Total Environ. 649, 1260–1268.

Zhou, H., Lian, L., Yan, S., Song, W., 2017. Insights into the photo-induced formation of reactive intermediates from effluent organic matter: the role of chemical constituents. Water Res. 112, 120–128.

Zhou, Z., Zhou, M., Yang, X., Niu, J., Meng, F., 2018. Sunlight irradiation triggers changes in the fouling potentials of natural dissolved organic matter. Sci. Total Environ. 627, 227–234.